# Ovarian cancer cell–derived migration inhibitory factor enhances tumor growth, progression, and angiogenesis

**Thorsten Hagemann, Stephen C. Robinson, Richard G. Thompson, Kellie Charles, Hagen Kulbe, and Frances R. Balkwill**

Centre for Translational Oncology, Institute of Cancer and Cancer Research United Kingdom Clinical Cancer Centre, Barts and The London, Queen Mary's Medical School, London, United Kingdom

## Abstract

In view of our previous findings that tumor cell–derived macrophage migration inhibitory factor (MIF) increased macrophage-mediated ovarian cancer cell invasiveness *in vitro*, we investigated the wider significance of ovarian cancer cell–derived MIF for tumor growth, metastasis, and angiogenesis. We found that MIF is expressed in borderline and malignant ovarian tumors, and active MIF is found in malignant ascitic fluid. We next investigated the expression and function of MIF in a syngeneic ovarian cancer model. Stable knockdown of MIF in the murine ovarian cancer cell line ID8 decreased *in vivo* tumor burden and overall survival. Tumors arising from MIF knockdown cells had decreased proliferation and significantly increased apoptosis. This was associated with an increased phosphorylation of p53 and reduced Akt phosphorylation. MIF knockdown led to a changed cytokine profile in the ascitic microenvironment; tumor necrosis factor-α, interleukin-6 (IL-6), and IL-10 expression were all significantly decreased. Accompanying this decrease in cytokine expression was a significant decrease in macrophage infiltration into ascites. Additionally, MIF knockdown reduced the expression of proangiogenic cytokines vascular endothelial growth factor and keratinocyte chemoattractant (KC) and reduced the amount of endothelial cells in the malignant ascites. We conclude that autocrine production of MIF by ovarian cancer cells stimulates other cytokines, chemokines, and angiogenic factors that may promote colonization of the peritoneum and neovascularization of tumor deposits. [Mol Cancer Ther 2007;6(7):1993–2002]

**Note:** T. Hagemann and S.C. Robinson contributed equally to this work.

**Requests for reprints:** Thorsten Hagemann, Centre for Translational Oncology, Institute of Cancer and Cancer Research United Kingdom Clinical Cancer Centre, Barts and The London, Queen Mary's Medical School, John Vane Science Centre, Charterhouse Square, London EC1M 6BQ, United Kingdom. Phone: 44-20-78826108; Fax: 44-20-78826110. E-mail: t.hagemann@qmul.ac.uk

## Introduction

Inflammation is key to the integrity and survival of multicellular organisms, but deregulation of this powerful component of the immune system is a characteristic of many chronic pathologies including cancer (1, 2). Inflammatory processes can promote, or maybe even initiate, malignant disease (3–6). One group of molecules that seem to be crucial in generating a proinflammatory tumor-promoting milieu are cytokines such as tumor necrosis factor-α, interleukin-1 (IL-1), and IL-8. Upstream of, or in a network with, these mediators is another influential cytokine, macrophage migration inhibitory factor (MIF).

MIF was one of the first cytokine activities to be described (7, 8), originally being identified as a product of activated T lymphocytes that inhibited the random migration of cultured macrophages. As with many other cytokines, other activities were soon ascribed to MIF, and a peptide released by the anterior pituitary gland in response to stress was identified as MIF (9). It is now clear that MIF is a key regulator of immune and inflammatory responses and is produced by a range of cells and tissues. Subsequent studies of MIF expression *in vivo* have established an important role in host response to endotoxic shock (10) and the inflammatory pathologies responsible for arthritis (11). MIF is a key inducer of inflammatory cytokines such as tumor necrosis factor-α (TNF-α) and IL-1 (10) and macrophages from *Mif* knock-out mice have a severely diminished TNF-α response to bacterial endotoxin both *in vitro* and *in vivo* (12). Recent studies describe the existence of a MIF-glucocorticoid counterregulatory system that controls inflammation and immune response (13), and released MIF can supersede the glucocorticoid immunosuppressive effects (14). MIF binds to the extracellular domain of CD74, the cell-surface form of the MHC class-II–associated invariant chain (15). CD74 may be the long sought-after MIF receptor or a docking molecule that is implicated in the presentation of MIF to its so-far-unidentified receptor.

MIF expression is increased during the evolution of several malignancies (16). MIF has also been implicated in the angiogenic switch of early cancer (17), and we reported earlier a role for MIF in macrophage-induced ovarian cancer cell invasiveness (18). MIF also has the ability to protect tumor cells from apoptosis. An early observation came from

Hudson et al. (19) that MIF is capable of functionally inactivating the tumor suppressor p53. Mitchell et al. (20) showed that MIF also sustains macrophage survival and function by suppressing p53-dependent apoptosis and restores the proinflammatory function.

In this paper, we have studied the mechanisms through which malignant cell-derived MIF influences ovarian cancer growth. We found that ovarian carcinomas and malignant ascites of ovarian cancer patients express MIF protein and activity. Knocking down MIF by RNAi in a murine epithelial ovarian cancer cell line, ID8, we significantly reduced tumor growth and increased overall survival in a syngeneic model of ovarian cancer. Furthermore, knocking down MIF in ID8 cells changed a range of inflammatory mediators (TNF-α, IL-6) in the malignant ascites as well as the proangiogenic cytokine [vascular endothelial growth factor (VEGF), KC].

This protumor cytokine milieu is likely to stimulate a continuing chemical conversation between the developing tumor and its supportive stroma (3). However, some cytokines are critical to the maintenance of this pathologic network, as seen by the activity of TNF-α antagonists in inflammatory diseases. We show that targeting MIF may also provide a valuable tumor therapy by targeting the proinflammatory cytokine network in ovarian cancer.

## Materials and Methods

### Cells Lines and Reagents

The IGROV-1 (21) and the TOV21G (American Type Culture Collection) human ovarian cancer cell lines were cultured in RPMI 1640 supplemented with 10% fetal bovine serum. The murine ovarian cancer cell line ID8 (22) was cultured in DMEM supplemented with 4% fetal bovine serum (FBS) and insulin (5 μg/mL), transferrin (5 μg/mL), and sodium selenite (5 ng/mL; all from Sigma). All experiments were done under endotoxin-free conditions. Cell viability and proliferation were measured using the Beckham Coulter ViCell XR Counter.

### Akt pThr[308] and pSer[473] ELISA Detection

We used the PhosphoDetect Akt (Ser[473] and Thr[308]) ELISA kit. These kits are designed to detect and quantify the level of Akt protein that are phosphorylated at serine residue 473 or threonine residue 308. We used whole tumor lysates for the detection of Akt following the manufacturer's instructions. Plates were read in a Dynatech MR 5000 plate reader at 450 nm.

### DNA-Binding Activity of HIF-1α Transcription Factor

An ELISA-based signaling assay (TransFactor, Becton Dickinson) was used to identify HIF-1α transcription factor activity in tumor lysates. The plates were read in a Dynatech MR 5000 plate reader at 650 nm.

### Patient Samples

Collection of ascitic fluid and solid tumors was approved by the East London and City Health Authority Research Ethics Committee and the local ethics committee of the University Hospital Göttingen. Samples of ascitic fluid were collected from patients who had ovarian carcinoma at the time of surgery or by paracentesis for palliative/diagnostic purposes or from patients with liver cirrhosis who needed diagnostic paracentesis. Each sample was centrifuged, and the ascitic fluid was removed for analysis.

### Mice

All mice were housed in negative-pressure isolation at the Cancer Research United Kingdom containment facility. In every experiment, we used 8-week-old wild-type C57Bl/6 background female mice (age matched within 3 days).

### ID8 Tumor, MIF RNAi ID8 Tumors

ID8 cells were transfected with pSilencer2.1-U6puro RNAi plasmids (Ambion) for MIF or a control plasmid containing scrambled RNA (mock). Cells were transfected using LipofectAMINE 2000 (Invitrogen) following the manufacturer's instructions. Antibiotic selection for stable cell lines started after 48–72 h in 4 μg/mL puromycin (Sigma) for 30 days. The syngeneic ID8, ID8-MIF RNAi, or ID8-mock murine ovarian cancer cell line (ID8-mock and ID8 MIF RNAi cells were a pool of clones) was grown in female C57Bl/6 mice. ID8 cells ($5 \times 10^6$) in 0.1 mL of PBS were injected i.p. Ascites and solid tumors were collected and fixed in 10% formal saline, liquid nitrogen, or used for fluorescence-activated cell sorting (FACS) analysis.

### Quantification of Tumor Blood Vessels

To visualize the architecture of blood vessels, animals were anesthetized using isoflurane, injected with FITC-conjugated tomato lectin (100 μL, 2 mg/mL, Vector Laboratories) via the tail vein. The lectin was allowed to circulate for 3 min before animals were perfused with 4% paraformaldehyde. Following fixation, resected primary tumors were isolated, cryoprotected in 12%, 15%, and 18% sucrose in PBS for 30 min each at 4°C, and snap-frozen in optimal cutting temperature compound (Sankura Finetek). Tumors were cut into 50-μm sections. Cell nuclei were stained using 4′,6-diamidino-2-phenylindole (DAPI, 200 ng/mL, Vector Laboratories), vessels were visualized using confocal microscopy (Zeiss LSM 510 META), and microvessel density was quantified using ImagePro Plus software (Image-Pro plus, Media Cybernetics). Vessel density was expressed as the mean percentage of total surface area.

### Assay for *p*-Hydroxyphenylpyruvate Tautomerase Activity

Measurement of *p*-hydroxyphenylpyruvate (HPP) tautomerase activity was done as described previously (17). Briefly, tissue or cell lysate (200 μL) or rMIF was added to a quartz cuvette containing 10 μL of 100 mmol/L HPP in 300 μL of 0.435 mol/L boric acid (pH, 6.2) and 690 μL of distilled water. The increase in absorbance (OD) at 330 nm between 10 and 40 s at 25°C was measured ($A_{33010-40s}$), and the value was corrected for the background $A_{33010-40s}$ value in the presence of PBS only. The HPP tautomerase activity of cell or tissue homogenate supernatants or ascites was expressed as $A_{33010-40s}$ per milligram of total protein. The presence of protease inhibitors in the lysis buffer did not affect HPP tautomerase activity in homogenates.

### RNA Extraction and Transcription

RNA was extracted using the ABI PRISM 6700 automated nucleic acid workstation (Applied BioSystems) according to

the manufacturer's protocol. RNA (2 µg) was reverse transcribed into 100 µL cDNA using Moloney murine leukemia virus reverse transcriptase and random hexamers (Promega).

### Real-Time PCR Low-Density Array

Gene expression comparisons between control macrophages, macrophages from ID8-MIF RNAi-bearing mice, or anti–MIF-treated mice were done using low-density array for 96 genes in duplicate (Applied BioSystems) on an ABI 7900HT genotyper using SDS2.1 software. The expression level of each gene was normalized to 18S and calibrated to control sample to obtain the relative expression level. Each gene was assessed in duplicate in every experiment, and only the genes with reproducible amplification curves were analyzed. Experiments were carried out in triplicate.

### Western Blotting and Immunoprecipitation

Whole-cell lysates from tumors were prepared, and Akt phosphorylation was measured after immunoprecipitation with anti-Akt antibody, using the following antibodies: anti-Akt pSer[473] and pThr[308] (all Cell Signaling). Normalized cell homogenates were prepared by boiling with one quarter volume of concentrated Laemmli sample buffer (100°C, 5 min). Cell extracts (10 µg) were resolved on a 10% denaturing gel using running buffer [25 mmol/L Tris; 192 mmol/L glycine, 0.1% (w/v) SDS]. See-Blue markers (Invitrogen Ltd.) were used to determine protein size. Antibody hybridizations were done according to the manufacturer's protocol. Antibodies used were anti-human MIF (clone 12302, R&D Systems), anti-mouse MIF (Abcam), and p53 and phosphorylated p53 (Ser[15]; Cell Signaling).

Proteins were visualized using the enhanced chemiluminescence reagent (Amersham). Protein concentration equivalence was confirmed by β-actin (Sigma) Western blot.

### Flow Cytometry

Murine Fc receptors were blocked using anti-mouse CD16/CD32 (mouse Fc Block, BD PharMingen). For staining, cells were washed and resuspended in PBS supplemented with 1% heat-inactivated FBS and 0.01% NaN$_3$. Antibodies were diluted in this buffer and used at a final concentration of between 2 and 20 µg/mL. Antibodies used were T cells CD4-FITC, CD8-PE, and CD45-APC; Treg cells CD4-FITC, Foxp3-PE, and CD25-APC; B cells B220-FITC, CD19-PE, and CD45-APC; γδT cells TCRγδ-FITC, and CD45-APC; neutrophils Gr-1-FITC and CD45-APC; endothelial cells CD31-FITC; natural killer (NK)/T cells NK1.1-FITC, and DX5-PE; macrophages F4/80-FITC, CD11b-PE, and CD45-APC; and dendritic cells CCR-7-FITC, CD80-PE, and CD11c-APC. Incubations with antibodies were carried out for 30 min on ice. Following the final washing step, labeled cells were analyzed by flow cytometry on a FACScan flow cytometer using Cellquest software (Becton Dickinson).

### Histology and Immunohistochemistry

Tumors for histologic analysis were harvested from time-matched animals at the end of observation, fixed in buffered formalin, and embedded in paraffin. Tissue slices (5 µm) were stained using H&E. General tissue morphology was visualized by H&E. Human and mouse MIF staining was carried out as described before (17). Mouse monoclonal
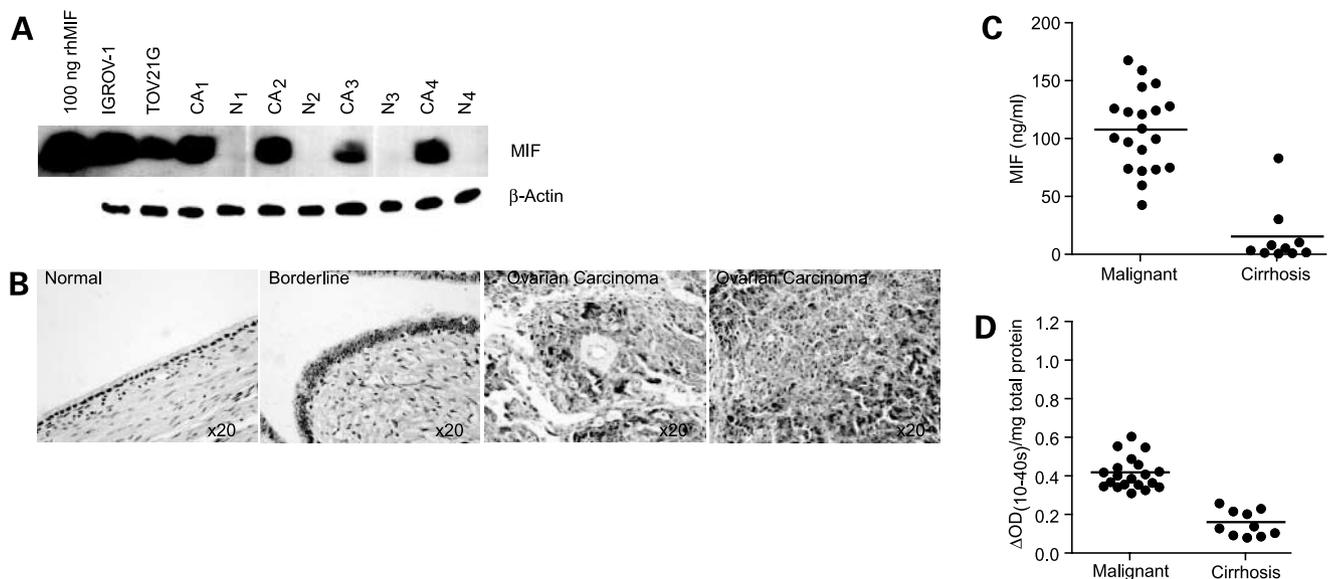


**Figure 1.** **A,** Western blot analysis of MIF (12.5 kDA) and β-actin (42 kDA) protein in paired human normal (*N*) and ovarian carcinomas (*CA*) and the human ovarian cancer cell lines IGROV and TOV21G. Representative data are shown for 4 of 10 pairs. *Left,* 100 ng of rhMIF. **B,** localization of MIF expression in normal human ovarian surface epithelium, borderline, and ovarian carcinoma by immunohistochemistry. *Left to right,* normal ovarian surface epithelium. No immunoreactivity in surface epithelium. MIF is present in ovarian borderline malignancies. Increased MIF immunoreactivity in ovarian carcinomas. **C,** MIF protein levels in 20 malignant (ovarian carcinoma) and 10 benign ascites (*n* = 10 cirrhosis) samples measured by ELISA. **D,** tautomerase activity for correlates with MIF protein expression.
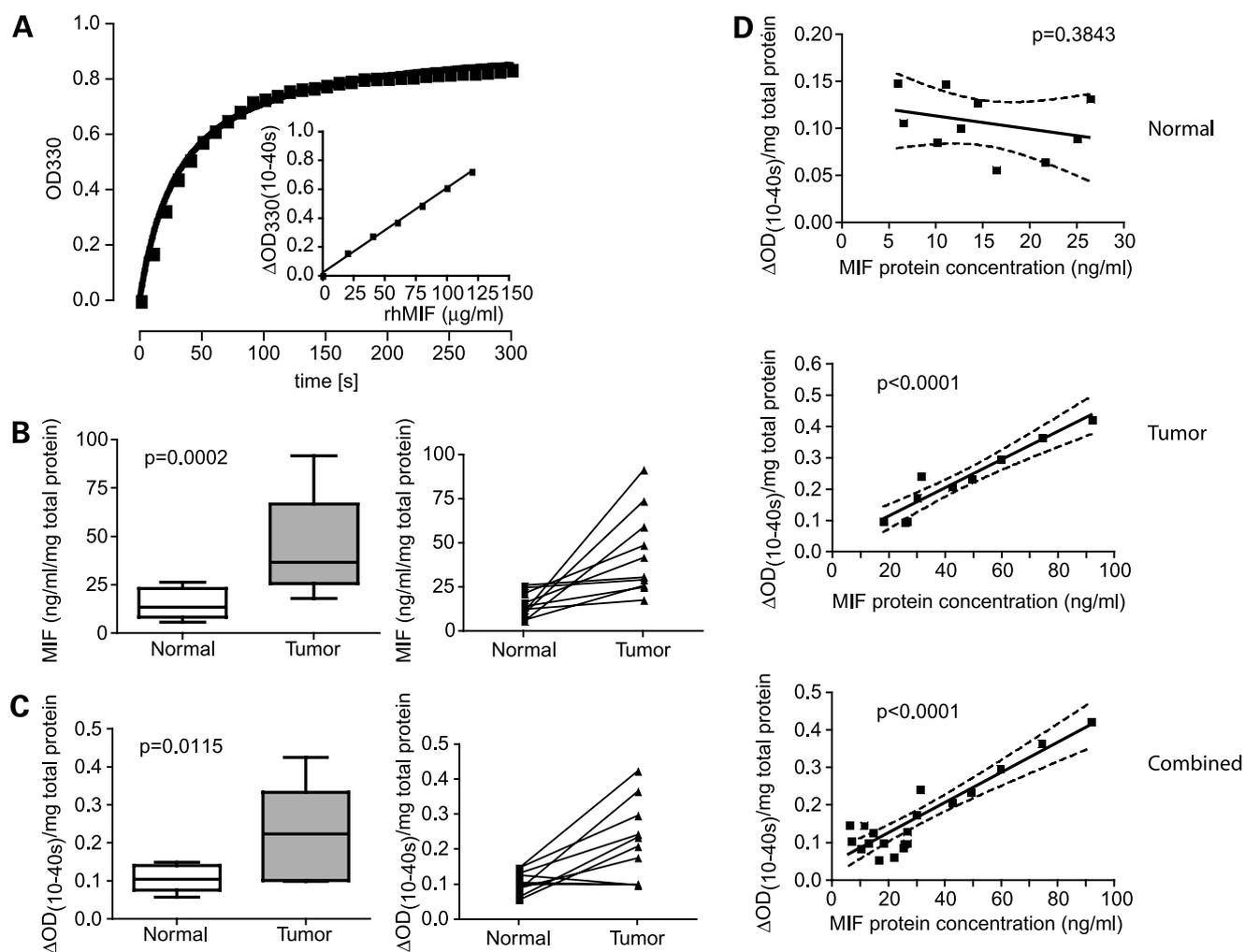
**Figure 2.** **A,** the change in $A_{330}$ after the addition of 1.2 μg of rhMIF to the HPP automerase assay. The change in $A_{330}$ between 10 and 40 s ($A_{33010\text{-}40s}$) was used as readout of HPP tautomerase activity in ovarian tissue homogenates after confirmation that there was a strict linear relationship between $A_{33010\text{-}40s}$ and the amount of MIF protein present (*inset*). **B,** MIF protein levels in 10 paired normal ovarian tissue and carcinoma tissue samples measured by ELISA. Lines join individual paired values. **C,** HPP tautomerase activity in the same 10 paired normal and carcinoma tissue samples. Lines join individual paired values. **D,** linear regression for tautomerase activity in normal tissue samples, ovarian cancer samples, and combined data for normal and ovarian cancer samples. Tautomerase activity distinguishes between normal and malignant tumor samples.

antihuman MIF antibody (1 mg/mL; R&D Systems) was incubated with sections for 2 h at 25°C. Negative controls used included omission of the primary antibody, incubation with 1 μg/mL irrelevant isotype control mouse IgG$_1$ (Sigma), and preadsorption of the primary antibody with 10 μg/mL rhMIF (R&D Systems) overnight at 4°C, before incubation with sections. To assess the tumor cellular proliferation (%Ki-67 positivity), immunohistochemical staining was done using the anti-mouse Ki-67 antigen (DAKO) and counterstained with H&E. Ki-67 staining was quantified by counting the number of positively stained cells of 200–250 nuclei in 10 randomly chosen fields at ×20. To quantify apoptosis, terminal nucleotidyl transferase–mediated nick end labeling (TUNEL) assay was done using a commercially available *in situ* apoptosis detection kit (Promega). For the quantification of total TUNEL expres-

sion, the number of apoptotic cells was counted in 10 randomly selected fields (×40) as a percentage of total cells using the Nikon Labophot II microscope (Nikon).

**Cytokine Detection**

To determine cytokine levels in the ascites or cell culture supernatants, Meso Scale Discovery System multiplex assay were used for murine IFN-γ, IL-1β, IL-2, IL-4, IL-5, IL-10, IL-12, KC, and TNF-α according to the manufacturer's instructions. Murine IL-17, IL-6, and human MIF was detected using the R&D ELISA (R&D Systems). Murine MIF was detected using the Chemicon ELISA (Chandler's Ford).

**Statistical Analysis**

All experiments were done in triplicate, and representative data are shown. Results were tested for statistical significance using Student's *t* test and Mann-Whitney test

with GraphPad Prism Version 4.0c software. The Kaplan-Meier survival data were examined using log-rank analysis with GraphPad Prism Version 4.0c software.

## Results

### MIF Expression by Human Ovarian Cancer and Normal Ovaries

We have previously shown that the human ovarian cancer cell line IGROV-1 expresses MIF (18). In this study, we first investigated whether MIF protein expression was increased in human ovarian cancer cell lines and in human primary ovarian cancers, compared with normal ovary tissue. Using Western blots, we found that MIF protein was detected in the human ovarian cancer cell lines (IGROV-1 and TOV21G) and was significantly increased in 12 human primary ovarian cancers compared with paired normal ovarian tissue (four representative samples shown, Fig. 1A). Immunohistochemstry showed MIF expression in borderline (10/10) and ovarian carcinoma (10/10), but not in normal ovarian surface epithelial (0/10; representative staining shown, Fig. 1B).

### MIF Protein Content of Malignant Ovarian Ascites

We assessed the MIF protein secretion into ascites of different pathologic origins. We analyzed malignant (from ovarian cancer patients) and cirrhotic (sterile) ascites (each group $n = 10$) and showed that MIF secretion is significantly higher in malignant compared with cirrhotic ascites (mean $\pm$ SD, malignant versus cirrhosis: 108.1 $\pm$ 34.28 ng/mL versus 15.82 $\pm$ 25.69 ng/mL, $P = 0.0001$; Fig. 1C). This increase in MIF protein correlated with MIF tautomerase activity (Fig. 1D).

MIF can catalyze tautomerization of several substrates, including HPP (17, 23), an activity that has previously been used as a measure of MIF activity *in vitro* (24). Therefore, we compared HPP tautomerase activity in normal and malignant human ovarian cancer protein lysates. First, we investigated the time course of the change in absorbance at 330 nm ($A_{330}$) induced by rhMIF in the HPP tautomerase assay (Fig. 2A). We chose a time point (40 s) during the period of linear increase in $A_{330}$ and then confirmed that the $A_{33010-40s}$ was directly proportional to the amount of rhMIF added (Fig. 2A, *inset*). HPP tautomerase activity was present in all 10 paired ovarian tissue homogenates that were tested (Fig. 2B, *right*, paired samples), and MIF tautomerase activity was significantly higher in carcinoma tissue compared with paired normal ovary tissue (Fig. 2C, *right*, paired samples; $P = 0.0115$ Mann-Whitney test). There is a significant linear regression between MIF protein and MIF tautomerase activity in tumor samples ($P < 0.0001$; Fig. 2D). This linear regression holds up even in the combined data from malignant and nonmalignant ascites and shows that tautomerase activity can distinguish between malignant and nonmalignant samples.

### Stable Knockdown of MIF in Syngeneic Ovarian Cancer Cells *In vitro*

Having shown that MIF protein and tautomerase activity were increased in human ovarian cancers compared with normal ovarian tissue, we next sought to investigate the effect of tumor cell–derived MIF *in vivo* by generating a variant of the murine ovarian cancer cell line, ID8 (22), that had stable expression of MIF shRNAi. The ID8 MIF RNAi cell line showed no differences in cell viability and proliferation compared with the parental cell line or a mock-transfected (scrambled shRNAi) line *in vitro* (Fig. 3A). The MIF shRNAi–expressing ID8 cells showed a significant down-regulation of MIF protein ($P < 0.001$) compared with the ID8-scrambled shRNAi cell line (Fig. 3B). Using a low-density RNA array (cytokines, chemokines, angiogenesis, and growth factors), we screened the MIF RNAi ID8 cell line (mixture of all three clones) for differences in RNA expression profiles (Supplementary data 1).[1] We found the mRNA expression of several chemokines (e.g., CCL2, CCL17, CCL19, CCL22) and cytokines (e.g., IL-10, IL-6, TNF-α) down-regulated in the MIF knockdown clones (Supplementary data 1).[1] However, there was a significant up-regulation of several chemokines as well as caspase-3, caspase-7, and p53.

### Effects of MIF Knockdown *In vivo*

ID8, ID8-scrambled shRNAi (mock), and ID8 MIF shRNAi–expressing cells were injected into female C57Bl/6 mice. Combined results from two separate experiments
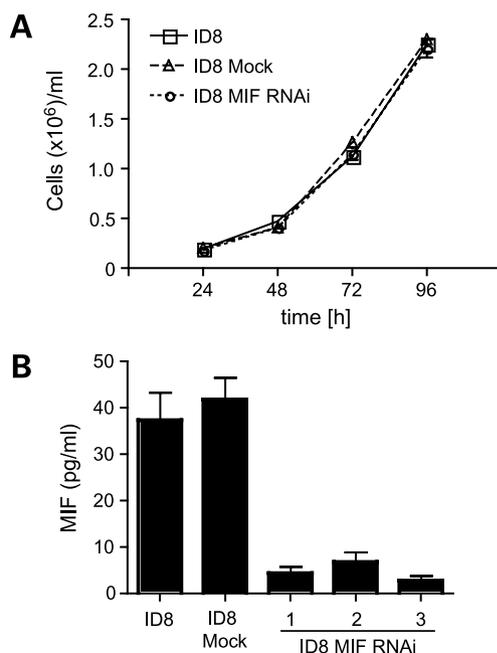


**Figure 3.** **A,** *in vitro* cell proliferation under reduced conditions. There is no growth advantage between the parental, mock-transfected, or MIF RNAi cell lines. **B,** in these experiments, ID8 mock cells are compared with three independently isolated MIF RNAi clones (1 – 3). MIF protein secretion as measured using ELISA after 72 h, mean values ($\pm$ SD) from triplicate wells. Silencing MIF expression by RNAi in ID8 cells results in decreased MIF protein secretion compared with ID8 mock or ID8 parental.

MIF knockdown was sustained *in vivo* as measured by ELISA of tumor cell lysates at the survival end point. Lysates from parental ID8 tumors contained an average of 167.6 ± 62.66 pg MIF/100 μg protein compared with 177.9 ± 56.63 pg MIF/100 μg protein in lysates from ID8 mock tumors and 62.09 ± 39.79 pg MIF/100 μg protein in lysates from MIF RNAi tumors (parental versus mock: $P = 0.6991$; parental versus MIF RNAi: $P = 0.0087$; mock versus MIF RNAi: $P = 0.0087$; Fig. 4D).

Next, we measured MIF protein and MIF tautomerase activity in the ascites. MIF tautomerase activity was assessed as described above and showed a significant reduction of MIF activity in ascites of MIF RNAi (mean ± SD, 0.09 ± 0.06) compared with ascites of scrambled RNAi (mean ± SD, 0.23 ± 0.98; $P = 0.003$) or parental ID8-bearing mice (mean ± SD, 0.2 ± 0.09; $P = 0.01$; Fig. 4D).

We assessed different cytokines and angiogenic factors in the ascites from tumor-bearing mice. Ascites from MIF RNAi ID8 tumor-bearing mice expressed significantly lower concentrations of the angiogenic factors KC and VEGF. MIF, IL-6, and TNF-α expression were also significantly lower in the ascites of mice bearing MIF RNAi ID8 tumors compared with ascites from parental or mock ID8 tumor-bearing mice (Table 1). The expression of IL-12 was significantly higher in MIF RNAi compared with parental or shRNAi ID8 tumor-bearing mice. There were no differences in IL-5, IL-10, and IL-17 protein expression. IL-1β, IL-2, IL-4, and IFN-γ expression could not be detected in the ascites (Table 1).

### Cellular Composition of Ascites in MIF Knockdown ID8-Bearing Mice

The cellular composition of the ascites was analyzed using FACS. There were no differences in neutrophil, T and B cell, Treg cell, and NK/T and dendritic cell infiltrate between the different groups. However, ascites of MIF RNAi ID8-bearing mice (mean ± SD, 6.29 ± 0.714%) showed a significant reduction (parental versus MIF RNAi ID8: $P = 0.007$; mock versus MIF RNAi ID8: $P = 0.0148$) in the proportion of endothelial cells compared with ID8- (parental, 14.74 ± 2.51%) and mock ID8 (13.96 ± 2.245%)–

bearing mice. Additionally, MIF RNAi ID8-bearing mice (mean ± SD, 8.7 ± 3.075%) had a significantly lower (parental versus MIF RNAi ID8: $P < 0.0001$; mock versus MIF RNAi ID8: $P = 0.0005$) macrophage ascitic infiltrate compared with ID8- (parental, 19.61 ± 3.17%) or mock ID8 (18.33 ± 5.236%)–bearing mice.

### MIF Knockdown Inhibits Angiogenesis *In vivo* and Inhibits Endothelial Cell Migration *In vitro*

FITC-lectin analysis of functional blood vessels showed a significant reduction of vascular area in tumors of mock compared with MIF RNAi ID8-bearing mice (Fig. 5A; $P < 0.0001$). In each group, mean vascular area of five tumors of matched size, taken from two different experiments, was assessed. In addition to the observed decrease in endothelial cells in MIF RNAi ID8 tumors, these data suggest that MIF may have a role in the formation of neovasculature.

### MIF Knockdown Inhibits Akt Phosphorylation and Increases p53 Phosphorylation

There is evidence that MIF prevents apoptosis via a pathway that involves Akt activation (25). We therefore investigated if Akt activation was affected in our *in vivo* tumors. In each group, we chose six tumors of matched size, taken from two different experiments, and assessed the phosphorylation of Akt at Ser[473] and Thr[308] using an ELISA-based assay. Tumors from the parental ID8 cell line (mean ± SD, 71.11 ± 21.89 units/mL) or mock ID8 tumors (70.75 ± 16.91 units/mL) had significantly higher levels of phosphorylated Akt pSer[473] compared with MIF RNAi tumors (41.36 ± 11.01 units/mL; $P < 0.05$; Fig. 5B). We analyzed Akt pThr[308] phosphorylation in the same samples. There was a significantly higher expression of Akt pThr[308] in tumors arising from the parental ID8 cells (mean ± SD, 52.64 ± 13.64 units/mL) or mock ID8 tumors (57.45 ± 10.98 units/mL) compared with MIF RNAi tumors (33.30 ± 8.865 units/mL; $P < 0.05$; Fig. 5B). Immunoprecipitation of total Akt and immunoblot against phosphorylated Akt pSer[473] and Akt pThr[308] confirmed the ELISA results (Fig. 5C).

MIF has recently been shown to interact and stabilize HIF-1α. In a similar approach as mentioned above, we

**Table 1.** Protein expression pattern (pg/mL) assessed in the ascites of tumor-bearing mice as measured using ELISA or Meso Scale multiplex assay

|  | Parental (pg/mL) | Mock (pg/mL) | MIF RNAi (pg/mL) | *P* value (parental versus MIF RNAi/mock versus MIF RNAi) |
|---|---|---|---|---|
| KC | 421.6 ± 80.42 | 510.3 ± 85.64 | 101.3 ± 77.29 | 0.0076/0.0036 |
| VEGF | 499 ± 112.6 | 444.3 ± 113 | 192.4 ± 48.56 | 0.0123/0.0239 |
| MIF | 188.4 ± 24.35 | 169.5 ± 18.01 | 51.37 ± 27.79 | 0.003/0.0035 |
| TNF-α | 174.9 ± 44.06 | 214.8 ± 53.43 | 90.5 ± 15.07 | 0.0349/0.0179 |
| IL-6 | 67.07 ± 17.72 | 78.2 ± 23.86 | 10.83 ± 2.684 | 0.0056/0.0083 |
| IL-5 | 3.536 ± 0.924 | 2.918 ± 1.106 | 3.881 ± 3.479 | 0.8762/0.6715 |
| IL-10 | 377.9 ± 88.85 | 396.9 ± 91.59 | 468.8 ± 115.4 | 0.3408/0.446 |
| IL-12 | 1,506 ± 62.95 | 1,309 ± 356.2 | 2,448 ± 62.16 | 0.0001/0.0055 |
| IL-17 | 86.3 ± 23.54 | 76.21 ± 31.52 | 83.21 ± 22.19 | 0.872/0.761 |

NOTE: Mean values (±SD, pg/mL) from three time-matched mice in each group are shown.
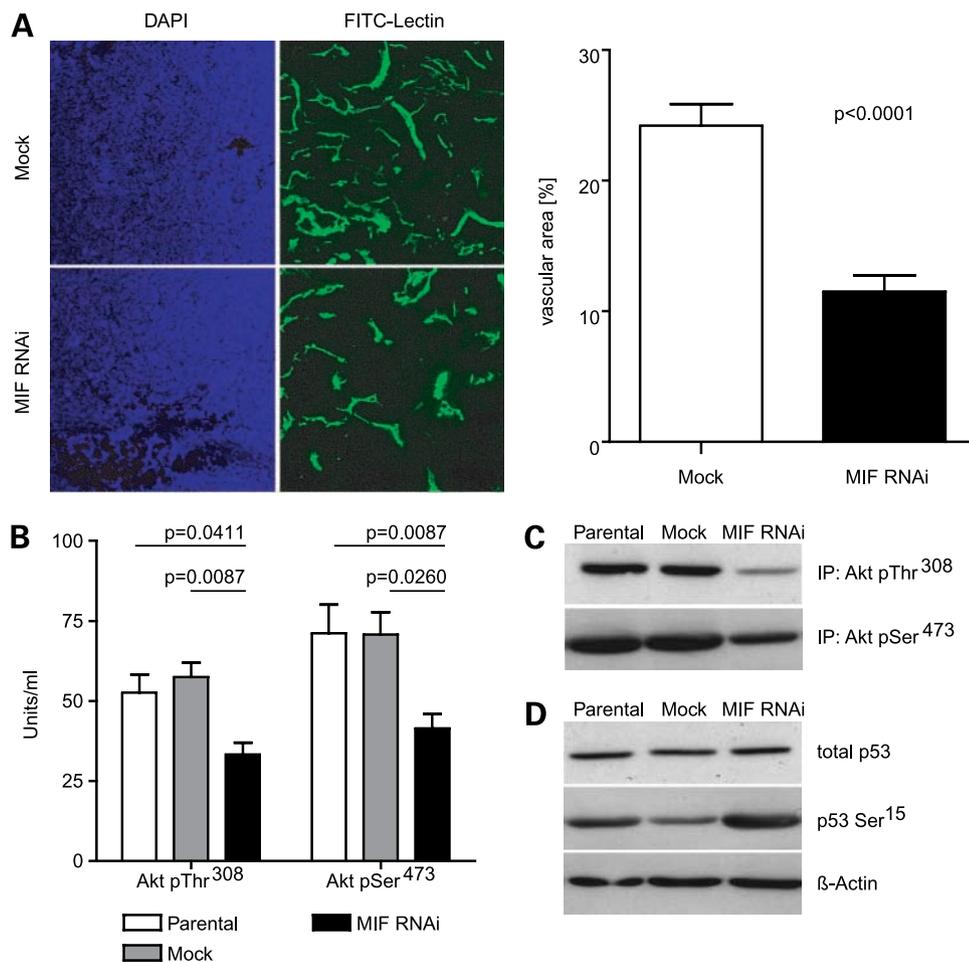
**Figure 5.** MIF activity *in vivo*. **A,** knockdown of MIF in ID8 cells results in significant reduced vascular area in time point–matched tumors ($P < 0.0001$). Vessels stained with FITC-lectin injection *in vivo*. **B,** Akt and p53 activation *in vivo*. Knockdown of MIF in ID8 cells results in significant reduced Akt phosphorylation *in vivo* in time point– and size–matched tumors. **C,** immunoprecipitation of Akt and immunoblot of phosphorylated Akt pSer$^{473}$ and Akt pThr$^{308}$. MIF RNAi tumors express less phosphorylated Akt compared with mock and parental ID8 tumors (representative blot shown). **D,** MIF RNAi tumors express higher phosphorylated p53 levels without any change in total p53 (representative blot shown).

analyzed the samples for differences in HIF-1α activity. There were no differences in HIF-1α activity between ID8 parental (mean ± SD, 0.872 ± 0.214 arbitrary units), mock ID8 (0.813 ± 0.288 arbitrary units), and MIF RNAi (0.843 ± 0.314 arbitrary units) tumor lysates.

Additionally, we analyzed the tumor lysates for p53 expression because it has been previously described that MIF could inhibit p53 suppressor activity (19). The tumor lysates from each group showed no differences in total p53 expression, but there was increased phosphorylated p53 in the MIF RNAi tumors compared with mock or parental ID8 tumors (Fig. 5D).

## Discussion

In this study, we present evidence that enhanced production of MIF by malignant ovarian epithelial cells supports ovarian cancer tumorigenesis. We show that autocrine secretion of MIF by ovarian cancer cells regulates the tumor microenvironment. The interaction with other cytokines, angiogenic factors, and chemokines may act in an autocrine/paracrine manner to promote tumor growth, progression, and neovascularization of ovarian cancer

deposits. The mechanisms of MIF action may include direct effects on malignant cell spread and cell survival via TNF-α and IL-6, immunosuppressive effects on leukocyte infiltrate via IL-10, and by stimulation of new blood vessels in the peritoneal tumor colonies due to the induction of KC and VEGF expression. Similar effects have been recently reported for TNF-α knockdown in a xenograft model of ovarian cancer (26) where TNF-α was shown to regulate MIF expression *in vivo*.

MIF expression has been reported in several tumors (16), but its role in ovarian cancer remains unclear. Increasing evidence has suggested that MIF contributes to tumorigenesis by inactivating p53 (19) and enhancing angiogenesis (17). We show that normal ovarian surface epithelium does not express MIF, but borderline and ovarian cancer does, suggesting that MIF may be a key protein in cancer. We observed significant increased amounts of MIF protein and MIF activity in both ovarian cancer samples and malignant ovarian ascites. In a human *in vitro* model of neoplastic progression where we irradiated an immortalized normal ovarian surface epithelial cell line, we found that during irradiation-induced accumulation of mutations, the expression and secretion

of MIF increases significantly.[2] This might lead to a synergistic effect together with the accumulation of p53 inhibition through p53 mutations. MIF inactivates the tumor suppressor p53 and, therefore, might directly inhibit tumor cell apoptosis (19). Additionally, this may provide a way to keep tumor-associated macrophages within the tumor environment where they may promote angiogenesis, tumor cell invasion, and growth. The MIF gene maps to chromosome 22q11.2 and a single nucleotide polymorphism (SNP; G to C transition) in the 5′-flanking region at position −173 of the MIF gene has been associated with susceptibility to adult inflammatory arthritis (27) and juvenile idiopathic arthritis (28). Therefore, it is of particular interest that in a population of ovarian cancer patients ($n$ = 1261), the expression of the minor C allele SNP was significantly ($P < 0.01$) increased compared with a normal, healthy population.[3] Women expressing the MIF SNP may be susceptible to ovarian cancer by either increased inhibition of p53-mediated apoptosis or by MIF-induced overexpression of cytokines such as TNF-α, IL-6, and reduced IL-12 expression.

The formation of new blood vessels is essential for tumor growth and is controlled by several angiogenic factors such as CXCL12 (26), IL-8 (human)/KC (murine; ref. 29), and VEGF (30), which are secreted by tumor cells and the surrounding stroma. Among these factors, VEGF is considered a crucial regulator for neovascularization and endothelial migration. Up-regulation of MIF has been shown to contribute to induced N-Myc expression by the activation of extracellular signal-regulated kinase signaling pathway and increased expression of IL-8 and VEGF in neuroblastomas (31). Our results, together with previously published data, suggest that VEGF is completed in a fine-tuned tumor microenvironment and regulated by MIF as well as TNF-α (26). A reduction in MIF levels *in vivo* had significant effects on the development of new blood vessels in the peritoneal tumor deposits. There are close interactions with at least three of the mediators released by ovarian tumor cells. MIF is an inducer of TNF-α (but also regulated by TNF-α; ref. 32) and VEGF (31); both molecules are able to induce CXCL12 (33, 34). TNF-α also directly induces CXCL12 and CXCL12 and VEGF synergized in the stimulation of neovascularization in ovarian cancer (35). VEGF expression is associated with increased angiogenesis, which, in turn, is correlated with increased metastasis of many cancers including ovarian cancer (36). TNF-α knockdown has a profound effect on survival in a xenograft model, including MIF and VEGF down-regulation (26). Our results, reported in a syngeneic model of ovarian cancer, are consistent with those of Kulbe et al. (26).

Wilson et al. (17) reported the crucial role of MIF for neovasculature in a murine model of colorectal cancer. Amin et al. (25) investigated the mechanism through which MIF induces angiogenesis. They found that MIF is a chemoattractant for endothelial cells and exhibit a protective role against endothelial cell apoptosis. MIF stimulation prevented endothelial cell apoptosis via a pathway that contained phosphoinositide-3-kinase and Akt, whereas mitogen-activated protein kinases were not involved. This is consistent with our results where we showed decreased Akt activity in tumor lysates from ID8 MIF RNAi-bearing tumors. Previously Winner et al. (37) showed that MIF is not only induced by hypoxia, but is also necessary for the maximal hypoxia-induced HIF-1α expression and stabilization. We found no differences in HIF-1α activity in ID8 MIF RNAi-bearing tumor lysates.

The actions of MIF display similarities with the one recently reported for TNF-α (26). MIF activity involve both the innate and adaptive immune response (12) in part due to the ability of MIF to antagonize the effects of glucocorticoids perhaps by preferential use of mitogen-activated protein kinase pathways (38). The role of MIF in the adaptive, T cell–driven, immune response is exemplified by the observation that immunoneutralization of MIF inhibits cutaneous delayed-type hypersensitivity reactions *in vivo* (39). In this perspective, the role of MIF within the tumor microenvironment could differ to its described role as a Th1 mediator. Together with the evidence for its tumor angiogenesis–promoting role, MIF attracts tumor-associated macrophages and is linked with increased TNF-α and IL-6 expression in the ovarian cancer microenvironment.

Our results suggest that targeting MIF and its angiogenic signaling pathway may be beneficial in the treatment of angiogenesis-dependent diseases.

### References

**1.** Balkwill F, Mantovani A. Inflammation and cancer: back to Virchow? Lancet 2001;357:539–45.

**2.** Coussens LM, Werb Z. Inflammatory cells and cancer: think different! J Exp Med 2001;193:F23–6.

**3.** Balkwill F, Charles KA, Mantovani A. Smoldering and polarized inflammation in the initiation and promotion of malignant disease. Cancer Cell 2005;7:211–7.

**4.** Greten FR, Eckmann L, Greten TF, et al. IKKβ links inflammation and tumorigenesis in a mouse model of colitis-associated cancer. Cell 2004; 118:285–96.

**5.** Pikarsky E, Porat RM, Stein I, et al. NF-κB functions as a tumour promoter in inflammation-associated cancer. Nature 2004;431:461–6.

**6.** Houghton J, Stoicov C, Nomura S, et al. Gastric cancer originating from bone marrow-derived cells. Science 2004;306:1568–71.

**7.** Bloom BR, Bennett B. Mechanism of a reaction *in vitro* associated with delayed-type hypersensitivity. Science 1966;153:80–2.

**8.** David JR. Delayed hypersensitivity *in vitro*: its mediation by cell-free substances formed by lymphoid cell-antigen interaction. Proc Natl Acad Sci U S A 1966;56:72–7.

**9.** Bernhagen J, Calandra T, Mitchell RA, et al. MIF is a pituitary-derived cytokine that potentiates lethal endotoxaemia. Nature 1993;365:756–9.

**10.** Calandra T, Echtenacher B, Roy DL, et al. Protection from septic shock by neutralization of macrophage migration inhibitory factor. Nat Med 2000;6:164–70.

___
[2] N.F. Li, personal communication.
[3] R. Payne, personal communication.

**11.** Leech M, Metz C, Santos L, et al. Involvement of macrophage migration inhibitory factor in the evolution of rat adjuvant arthritis. Arthritis Rheum 1998;41:910 – 7.

**12.** Calandra T, Roger T. Macrophage migration inhibitory factor: a regulator of innate immunity. Nat Rev Immunol 2003;3:791 – 800.

**13.** Calandra T, Bernhagen J, Metz CN, et al. MIF as a glucocorticoid-induced modulator of cytokine production. Nature 1995;377:68 – 71.

**14.** Bacher M, Metz CN, Calandra T, et al. An essential regulatory role for macrophage migration inhibitory factor in T-cell activation. Proc Natl Acad Sci U S A 1996;93:7849 – 54.

**15.** Leng L, Metz CN, Fang Y, et al. MIF signal transduction initiated by binding to CD74. J Exp Med 2003;197:1467 – 76.

**16.** Mitchell RA. Mechanisms and effectors of MIF-dependent promotion of tumourigenesis. Cell Signal 2004;16:13 – 9.

**17.** Wilson JM, Coletta PL, Cuthbert RJ, et al. Macrophage migration inhibitory factor promotes intestinal tumorigenesis. Gastroenterology 2005;129:1485 – 503.

**18.** Hagemann T, Wilson J, Kulbe H, et al. Macrophages induce invasiveness of epithelial cancer cells via NF-κB and JNK. J Immunol 2005;175:1197 – 205.

**19.** Hudson JD, Shoaibi MA, Maestro R, Carnero A, Hannon GJ, Beach DH. A proinflammatory cytokine inhibits p53 tumor suppressor activity. J Exp Med 1999;190:1375 – 82.

**20.** Mitchell RA, Liao H, Chesney J, et al. Macrophage migration inhibitory factor (MIF) sustains macrophage proinflammatory function by inhibiting p53: regulatory role in the innate immune response. Proc Natl Acad Sci U S A 2002;99:345 – 50.

**21.** Benard J, Da Silva J, De Blois MC, et al. Characterization of a human ovarian adenocarcinoma line, IGROV1, in tissue culture and in nude mice. Cancer Res 1985;45:4970 – 9.

**22.** Roby KF, Taylor CC, Sweetwood JP, et al. Development of a syngeneic mouse model for events related to ovarian cancer. Carcinogenesis 2000;21: 585 – 91.

**23.** Lubetsky JB, Swope M, Dealwis C, Blake P, Lolis E. Pro-1 of macrophage migration inhibitory factor functions as a catalytic base in the phenylpyruvate tautomerase activity. Biochemistry 1999;38: 7346 – 54.

**24.** Maaser C, Eckmann L, Paesold G, Kim HS, Kagnoff MF. Ubiquitous production of macrophage migration inhibitory factor by human gastric and intestinal epithelium. Gastroenterology 2002;122:667 – 80.

**25.** Amin MA, Volpert OV, Woods JM, Kumar P, Harlow LA, Koch AE. Migration inhibitory factor mediates angiogenesis via mitogen-activated protein kinase and phosphatidylinositol kinase. Circ Res 2003;93:321 – 9.

**26.** Kulbe H, Thompson R, Wilson JL, et al. The inflammatory cytokine tumor necrosis factor-α generates an autocrine tumor-promoting network in epithelial ovarian cancer cells. Cancer Res 2007;67:585 – 92.

**27.** Barton A, Lamb R, Symmons D, et al. Macrophage migration inhibitory factor (MIF) gene polymorphism is associated with susceptibility to but not severity of inflammatory polyarthritis. Genes Immun 2003;4: 487 – 91.

**28.** Donn R, Alourfi Z, Zeggini E, et al. A functional promoter haplotype of macrophage migration inhibitory factor is linked and associated with juvenile idiopathic arthritis. Arthritis Rheum 2004;50:1604 – 10.

**29.** Sparmann A, Bar-Sagi D. Ras-induced interleukin-8 expression plays a critical role in tumor growth and angiogenesis. Cancer Cell 2004;6: 447 – 58.

**30.** Carmeliet P, Jain RK. Angiogenesis in cancer and other diseases. Nature 2000;407:249 – 57.

**31.** Ren Y, Chan HM, Li Z, et al. Up-regulation of macrophage migration inhibitory factor contributes to induced N-Myc expression by the activation of ERK signaling pathway and increased expression of interleukin-8 and VEGF in neuroblastoma. Oncogene 2004;23:4146 – 54.

**32.** Morand EF, Leech M, Bernhagen J. MIF: a new cytokine link between rheumatoid arthritis and atherosclerosis. Nat Rev Drug Discov 2006;5: 399 – 410.

**33.** Jin DK, Shido K, Kopp HG, et al. Cytokine-mediated deployment of SDF-1 induces revascularization through recruitment of CXCR4 + hemangiocytes. Nat Med 2006;12:557 – 67.

**34.** Kaplan RN, Riba RD, Zacharoulis S, et al. VEGFR1-positive haematopoietic bone marrow progenitors initiate the pre-metastatic niche. Nature 2005;438:820 – 7.

**35.** Kryczek I, Lange A, Mottram P, et al. CXCL12 and vascular endothelial growth factor synergistically induce neoangiogenesis in human ovarian cancers. Cancer Res 2005;65:465 – 72.

**36.** Alvarez AA, Krigman HR, Whitaker RS, Dodge RK, Rodriguez GC. The prognostic significance of angiogenesis in epithelial ovarian carcinoma. Clin Cancer Res 1999;5:587 – 91.

**37.** Winner M, Koong AC, Rendon BE, Zundel W, Mitchell RA. Amplification of tumor hypoxic responses by macrophage migration inhibitory factor-dependent hypoxia-inducible factor stabilization. Cancer Res 2007;67:186 – 93.

**38.** Donnelly SC, Bucala R. Macrophage migration inhibitory factor: a regulator of glucocorticoid activity with a critical role in inflammatory disease. Mol Med Today 1997;3:502 – 7.

**39.** Bernhagen J, Bacher M, Calandra T, et al. An essential role for macrophage migration inhibitory factor in the tuberculin delayed-type hypersensitivity reaction. J Exp Med 1996;183:277 – 82.

# Molecular Cancer Therapeutics

## Ovarian cancer cell−derived migration inhibitory factor enhances tumor growth, progression, and angiogenesis

Thorsten Hagemann, Stephen C. Robinson, Richard G. Thompson, et al.

| | |
|---|---|
| **Updated version** | Access the most recent version of this article at:<br>http://mct.aacrjournals.org/content/6/7/1993 |

| | |
|---|---|
| **Cited articles** | This article cites 39 articles, 16 of which you can access for free at:<br>http://mct.aacrjournals.org/content/6/7/1993.full#ref-list-1 |
| **Citing articles** | This article has been cited by 12 HighWire-hosted articles. Access the articles at:<br>http://mct.aacrjournals.org/content/6/7/1993.full#related-urls |

| | |
|---|---|
| **E-mail alerts** | Sign up to receive free email-alerts related to this article or journal. |
| **Reprints and Subscriptions** | To order reprints of this article or to subscribe to the journal, contact the AACR Publications Department at pubs@aacr.org. |
| **Permissions** | To request permission to re-use all or part of this article, use this link<br>http://mct.aacrjournals.org/content/6/7/1993.<br>Click on "Request Permissions" which will take you to the Copyright Clearance Center's (CCC)<br>Rightslink site. |